ANTIOXIDANTS & REDOX SIGNALING
Volume 14, Number 1, 2011

DOI: 10.1089/ars.2009.3047

ORIGINAL RESEARCH COMMUNICATION

Hypoxia Induces Intracellular Ca^{2+} Release by Causing Reactive Oxygen Species-Mediated Dissociation of FK506-Binding Protein 12.6 from Ryanodine Receptor 2 in Pulmonary Artery Myocytes

Bo Liao,* Yun-Min Zheng,* Vishal R. Yadav, Amit S. Korde, and Yong-Xiao Wang

Abstract

Here we attempted to test a novel hypothesis that hypoxia may induce Ca^{2+} release through reactive oxygen species (ROS)-mediated dissociation of FK506-binding protein 12.6 (FKBP12.6) from ryanodine receptors (RyRs) on the sarcoplasmic reticulum (SR) in pulmonary artery smooth muscle cells (PASMCs). The results reveal that hypoxic exposure significantly decreased the amount of FKBP12.6 on the SR of PAs and increased FKBP12.6 in the cytosol. The colocalization of FKBP12.6 with RyRs was decreased in intact PASMCs. Pharmacological and genetic inhibition of intracellular ROS generation prevented hypoxia from decreasing FKBP12.6 on the SR and increasing FKBP12.6 in the cytosol. Exogenous ROS (H_2O_2) reduced FKBP12.6 on the SR and augmented FKBP12.6 in the cytosol. Oxidized FKBP12.6 was absent on the SR from PAs pretreated with and without hypoxia, but it was present with a higher amount in the cytosol from PAs pretreated with than without hypoxia. Hypoxia and H_2O_2 diminished the association of FKBP12.6 from type 2 RyRs (RyR2). The activity of RyRs was increased in PAs pretreated with hypoxia or H_2O_2. FKBP12.6 removal enhanced, whereas RyR2 gene deletion blocked the hypoxic increase in $[Ca^{2+}]_i$ in PASMCs. Collectively, we conclude that hypoxia may induce Ca^{2+} release by causing ROS-mediated dissociation of FKBP12.6 from RyR2 in PASMCs. *Antioxid. Redox Signal.* 14, 37–47.

Introduction

Hypoxia causes vasoconstriction in pulmonary arteries (PAs), termed hypoxic pulmonary vasoconstriction (HPV). The function of this unique cellular response is to maintain adequate oxygen exchange in the lungs, but chronic HPV can be a significant pathological factor in the development of pulmonary hypertension and even heart failure. HPV may result from an increase in intracellular Ca^{2+} concentration ($[Ca^{2+}]_i$) in PA smooth muscle cells (PASMCs). We and other investigators have shown that Ca^{2+} release from the sarcoplasmic reticulum (SR) through ryanodine receptors (RyRs) plays an important role in the hypoxic increase in $[Ca^{2+}]_i$ in PASMCs and HPV (3, 4, 7, 12, 13, 19, 25, 31, 32). The importance of RyRs in hypoxic responses in PASMCs is reinforced by findings that Ca^{2+} release from the SR is likely to inhibit voltage-dependent K^+ channels (15, 22) and to open store-operated Ca^{2+} channels (13, 14), which cause extracellular Ca^{2+} influx, thus providing a positive feedback mechanism to enhance the hypoxic increase in $[Ca^{2+}]_i$ and contraction.

Although the signaling mechanisms by which hypoxia activates RyRs in PASMCs are incompletely understood, RyRs may mediate hypoxic Ca^{2+} and contractile responses as a consequence of the increased generation of mitochondrial reactive oxygen species (ROS). Numerous reports have provided pharmacological and genetic evidence that mitochondrial ROS is responsible for the hypoxic increase in $[Ca^{2+}]_i$ in PASMCs and associated HPV (1, 24, 27). Exogenous ROS, mimicking hypoxia, also leads to an increase in $[Ca^{2+}]_i$ and contraction in PASMCs (8, 16–18, 26). Moreover, application of ryanodine to block RyRs significantly inhibits ROS-evoked increase in $[Ca^{2+}]_i$ in PASMCS (8). Supportively, the RyR antagonists dantrolene and ryanodine eliminate or greatly suppress ROS-induced increase in $[Ca^{2+}]_i$ and vasoconstriction in isolated PAs (16). Previous studies have shown that FK506-binding protein 12.6 (FKBP12.6) is associated with type 2 RyRs (RyR2) and inhibits these Ca^{2+} release channels in vascular SMCs (20, 30). We have further found that both chemical and genetic removal of FKBP12.6 can significantly enhance the hypoxic Ca^{2+} release in PASMCs and attendant

Center for Cardiovascular Sciences, Albany Medical College, Albany, New York.
*These authors contributed equally to this work.

HPV (30). These findings suggest that FKBP12.6 is involved in hypoxic cellular responses in PASMCs.

To elucidate the molecular processes by which FKBP12.6 may mediate the hypoxic increase in $[Ca^{2+}]_i$ in PASMCs, in this study we sought to address the following three fundamental questions: (1) Could hypoxia disassociate FKBP12.6 from RyR2 on the SR membrane? (2) Was the hypoxia-induced dissociation of FKBP12.6 from RyRs secondary to the increased mitochondrial ROS generation? and (3) Did the hypoxic dissociation of FKBP12.6 cause a significant increase in the activity of RyRs and associated Ca^{2+} release in PASMCs?

Materials and Methods

Materials

Anti-actin antibody, collagenase, dithiothreitol, dithioerythritol, hydrogen peroxide, myxothiazol, and ryanodine were purchased from Sigma-Aldrich Corp.; anti-calnexin, anti-FKBP12/12.6, and anti-RyR2 antibodies (Ab1093) from ABR Affinity Bio-Reagents Products; fura-2/AM from Molecular Probes; papain from Worthington Biochemical Corp.; and [^{3}H]-ryanodine from PerkinElmer Corp.

Preparation of isolated PA tissues and SMCs

All animal experiments were approved by the Institutional Animal Care and Use Committee of Albany Medical College. Isolated resistance (third or smaller branch) PA smooth muscle tissues and cells were prepared from Swiss-Webster mice (Taconic), as we previously described (30, 32). Mice were euthanized by an intraperitoneal injection of sodium pentobarbital. Resistance PAs with a diameter of 200 μm or less were carefully dissected free of endothelium and connective tissues in ice-cold, physiological saline solution (PSS) gassed with 20% O_2, 5% CO_2, and 75% N_2 (termed normoxia). To obtain isolated, single SMCs, dissected arteries were cut into small pieces and then incubated in low-Ca^{2+} (100 μM) PSS containing (mg/ml): 1.5 papain, 0.4 dithioerythritol, and 1.0 bovine serum albumin (BSA) for 20 min followed by low Ca^{2+} PSS containing (mg/ml): 1.0 collagenase II, 1.0 collagenase H, 1.0 dithiothreitol, and 1.0 BSA for 10–15 min. The digested PAs were gently triturated to harvest single SMCs. Glutathione peroxidase-1 (Gpx1) gene-deleted ($Gpx1^{-/-}$), Gpx1 gene-overexpressing (Gpx1-Tg), and $RyR2^{-/+}$ mice were generated and maintained, as we previously reported (9, 18, 23). Isolated PAs or PASMCs from $Gpx1^{-/-}$, Gpx1-Tg, $RyR2^{-/+}$ and corresponding control (wildtype) mice were obtained using the same protocol as just described.

Preparation of cell lysate, and isolated SR membrane as well as cytosol fractions

Dissected PAs were homogenized in homogenization buffer containing 0.29 *M* sucrose, 3 m*M* imidazole/HCl (pH 7.4), and a protease inhibitor mix (1 m*M* benzamidine, 2 μg/ml leupeptin, 2 μg/ml pepstatin A, 2 μg/ml aprotinin, and 0.5 m*M* phenylmethanesulphonyl fluoride) and then solubilized in lysis buffer containing 25 m*M* Tris, 50 m*M* HEPES (pH 7.4), 137 m*M* NaCl, 1% 3-[(3-cholamidopropyl) dimethylammonio]-1-propanesulfonic acid, 0.5% soya-bean phosphatidylcholine, 2.5 m*M* dithiothreitol, and the above-described protease inhibitor mix on ice for 1 h. The cell lysate was collected by centrifugation twice at 16,000 *g* for 30 min at 4°C.

To obtain SR membrane and cytosol fractions, the homogenate from isolated PAs was centrifuged at 1000 *g* for 20 min at 4°C. The pellet was re-homogenized and centrifuged. The supernatant was centrifuged at 27,000 *g* for 15 min at 4°C. Then the supernatant was ultra-centrifuged at 100,000 *g* for 15 min at 4°C to collect the supernatant as the cytosol fraction and the pellet as the SR membrane fraction.

Western blot analysis

Western blotting was performed using a similar procedure to that described in our earlier report (30). Protein concentrations in isolated SR membrane and cytosolic fractions were determined using the Protein Assay Reagent Kit (Pierce). The same amount (20 μg) of total proteins from isolated SR membrane and cytosolic fractions were loaded into wells in the sodium dodecyl sulfate–polyacrylamide gel electrophoresis (SDS-PAGE) gel and then transferred to a polyvinylidene fluoride (PVDF) membrane (Bio-Rad Laboratories). After transfer, the membrane was cut into two parts. The low part was blotted with an anti-FKBP antibody (1:800 dilution), and the top part was incubated with anti-actin antibody (1:2000 dilution) to further ensure equal protein loading. After incubation overnight at 4°C, the membranes were washed thrice for 10 min with Tris-buffered saline with Tween-20 (TBST) buffer (20 m*M* Tris, 150 m*M* NaCl, and 0.1% Tween 20) and then incubated with a horseradish peroxidase-conjugated secondary antibody (1:2500 dilution) for 1 h. The nonspecific binding sites on the membrane were blocked by TBST buffer containing 5% nonfat dry milk for 1 h. The separated parts of the membrane were placed together. Blots were visualized using a chemiluminescence detection kit (Santa Cruz Biotech). The blot band densities were quantified as numerical values in arbitrary units using Multi Gauge software version 3.0 (Fujifilm Science Systems). The numerical values of FKBP12.6 blot bands were divided by those of actin blot bands to represent the amount of FKBP12.6.

To determine the ratio of FKBP12.6 to calnexin, the PVDF membrane was first incubated with anti-FKBP antibody (1:800 dilution) and then stripped for incubation with anti-calnexin antibody (1:3000 dilution) overnight. The numerical values of FKBP12.6 and calnexin blot bands were obtained, as described above.

Double immunofluorescence staining

The experimental procedure was the same as that described in our previous reports (32). Freshly isolated cells were placed on coverslips precoated with fibronectin (40 μg/ml) in phosphate-buffered saline (PBS) for 30 min at room temperature, fixed using 4% paraformaldehyde for 15 min, and permeabilized with 0.2% Triton. After incubated in 2.5% BSA in PBS blocking solution for 30 min, cells were incubated with anti-FKBP12.6 antibodies (1:250 dilution) and anti-RyR antibodies (1:150) for overnight at 4°C, followed by Alexa488- and Alxa594-conjugated antibodies for 90 min. After cells were washed with 0.2% BSA solution in PBS, SlowFade Light Antifade Kit (Molecular Probes) was added. Immunofluorescence staining was examined using an LSM510 laser scanning confocal microscope (Carl Zeiss). Alexa488 and Alexa594 were excited at 488 and 543 nm using a krypton-argon laser and fluorescence detected using 505 and 585 nm bandpass filters, respectively. The *z* interval was

adjusted to 1 μm to obtain sufficient fluorescence signals. To quantify the colocalization of FKBP12.6 with RyRs, Zeiss Physiology version 3.2 software was used to obtain colocalization coefficients, which are calculated based on Pearson's correlation coefficient and adequately describe the degree of colocalization between two molecules (11).

FKBP12.6 and RyR2 oxidation detection

FKBP12.6 oxidation was determined by assessing ROS-mediated formation of carbonyls, which was detected by a reaction with 2, 4-dinitrophenyl hydrazine (DNPH) using an OxyBlot™ Protein Oxidation Detection Kit (Chemicon International, Inc.), as previously described (5). According to the manufacturer's instructions, 5 μl of soluble SR membrane or cytosol fraction samples were denatured by 5 μl 12% of SDS and then derivatized with 10 μl of 1× DNPH (20 m*M* DNPH in 10% trifluoracetic acid) for 15 min at room temperature. The derivatization reaction was stopped by adding 7.5 μl of neutralization solution (2 *M* Tris, 30% glycerol, and 19% β-mercaptoethanol). The derivatized proteins were electrophoresed on a SDS-PAGE gel and transferred onto a PVDF membrane. The membrane was incubated with an anti-DNP antibody (1:150 dilution) for ~1 h, washed three times with TBST, and incubated with a horseradish peroxidase-conjugated antibody for ~1 h. Blots were visualized and analyzed as described above. All samples were performed in duplicate.

To detect RyR2 protein oxidation, isolated SR membrane samples were incubated with an anti-RyR2 antibody (1:250 dilution) for 4 h at 4°C followed by protein A/G-agarose conjugate (25% v/v) for 2 h at 4°C, and then centrifuged at 1000 *g* for 30 s to collect immunoprecipitates. The immunoprecipitates were washed three times with radioimmunoprecipitation assay buffer and resuspended in 25 μl of 2× loading buffer. Immunoprecipitated RyR2 protein oxidation was assessed using the same procedure as described above.

Assay of FKBP12.6 coimmunoprecipitation by RyR2

Isolated SR membrane samples were incubated with protein-G sepharose (20 μl) that was prebound with 1 μl of an anti-RyR2 antibody at 4°C for 18 h. The immunoprecipitates were washed thrice for 10 min with ice-cold homogenization buffer containing a protease inhibitor mix and then eluted by adding 20 μl of 2× Laemmli sample buffer containing 5% β-mercaptoethanol. After the samples were boiled for 5 min, FKBP12.6 was separated by 5% SDS-PAGE, probed with an anti-FKBP antibody (1:800 dilution), and then visualized by a chemiluminescence detection kit.

[^{3}H]-Ryanodine binding assay

[^{3}H]-ryanodine binding assay was made as previously described (10). Briefly, cell lysate (90 μg protein) was incubated with [^{3}H]-ryanodine at 5–25 n*M* at 37°C for 3 h in a binding assay solution (300 μl) containing 25 m*M* Tris, 50 m*M* HEPES, a protease inhibitor mix, and 100 μ*M* $CaCl_2$ (pH 7.4). The binding mixture was diluted with ice-cold washing buffer (3 ml) containing 25 m*M* Tris (pH 8.0) and 250 m*M* KCl and immediately filtered through Millipore Membrane filters presoaked with washing buffer. The filters were washed three times with ice-cold washing buffer (5 ml). The radioactivity associated with the filters was determined by liquid scintillation counting. Nonspecific binding was determined in the presence of 50 μ*M* unlabeled ryanodine. All binding assays were executed in duplicate.

Intracellular ROS detection

Detection of intracellular ROS was conducted using the fluorescent ROS indicator 5,6-chloromethyl-2,7-dichlorodihydrofluorescein (DCF) diacetate, as was previously reported (17, 18, 23). Freshly isolated cells at 10^4 cells/well were loaded with 5,6-chloromethyl-DCF diacetate (5 μ*M*) in a 96-well plate at 37°C for 30 min. DCF-derived fluorescence was measured using a FlexStation-III microplate reader (Molecular Devices) with an excitation wavelength of 488 ± 20 nm and emission wavelength of 510 ± 20 nm. Intracellular ROS production was determined by the difference in DCF fluorescence between the wells containing the assay buffer with and without cells.

Measurement of $[Ca^{2+}]_i$

Measurement of $[Ca^{2+}]_i$ was made using a dual excitation wavelength fluorescence method (30), with either a TILLvisION digital imaging system (TILL Photonics GmbH) or FlaxStation-III microplate reader (Molecular Devices). Freshly isolated cells were loaded with the fluorescent Ca^{2+} indicator dye fura-2/AM (10 μ*M*) in normoxic PSS at room temperature for 30 min, followed by wash three times with dye-free PSS. The fluorescent dye was alternatively excited at 340 and 380 nm, and emitted fluorescence was detected at 510 nm. The background signal was corrected by the fluorescence recorded in either noncell regions or cells unloaded with fura-2/AM.

Hypoxia

To induce a hypoxic response, PA tissues or SMCs were exposed to a hypoxic PSS for 5 min. This time period was chosen, because our previous studies have shown that maximal cellular responses occur before or at 5 min after acute hypoxic exposure (7, 17, 18, 23, 30–32). In control experiments, tissues or cells were identically treated but exposed to a normoxic PSS. The normoxic and hypoxic PSS were made by gassing the solution with 20% O_2, 5% CO_2, and 75% N_2 and 1% O_2, 5% CO_2, and 94% N_2, respectively. The oxygen tension in the normoxic and hypoxic solutions was 140–150 and 10–20 Torr, as measured using an OXEL-1 oxygen electrode (World Precision Instruments).

Statistical analysis

Data are expressed as mean ± standard error of the mean of at least three independent experiments. Student's *t*-test or one-way analysis of variance with Bonferroni *post hoc* test was used to determine the significance of differences between comparisons. A $p < 0.05$ was accepted as statistically significant.

Results

Hypoxia causes translocation of FKBP12.6 from the SR membrane to the cytosol in PAs

Our previous study has shown that FKBP12.6 is involved in the hypoxic increase in $[Ca^{2+}]_i$ in PASMCs and associated HPV (30). As such, here we first sought to investigate whether the role of FKBP12.6 might occur due to its dissociation with

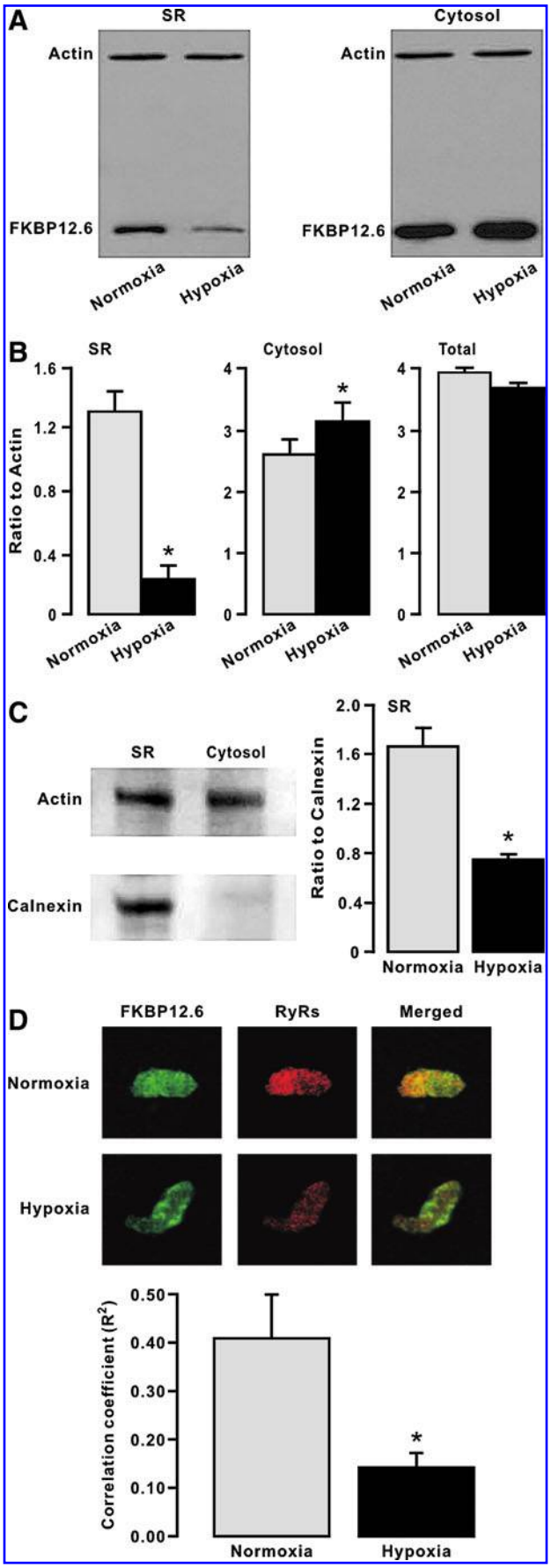

RyRs during hypoxic exposure. In these experiments, freshly isolated mouse PAs were first exposed to hypoxia for 5 min and then used to obtain the SR membrane and cytosol fraction. As control, the tissues were identically treated but exposed to normoxia instead. As shown in Figure 1A, after hypoxic exposure, the amount of FKBP12.6 was significantly reduced in the SR membrane fraction and correspondingly increased in the cytosol fraction. The amount of actin (loading control) was unchanged in either the SR membrane or cytosolic fraction. The ratio of FKBP12.6 to actin amount from three independent experiments is summarized in Figure 1B. We also found the total amount of FKBP12.6 was equivalent in whole lysates (including the SR membrane and cytosolic fractions) of PAs untreated and treated with hypoxia (Fig. 1B), indicating that the expression level of FKBP12.6 is unchanged after hypoxic exposure for 5 min. To verify successful isolation of the SR membrane fraction, we examined expression of the SR membrane resident protein calnexin. The results reveal that unlike actin, calnexin was present in the isolated SR membrane fraction but not in the cytosolic fraction (Fig. 1C). Further, the ratio of FKBP12.6 to calnexin amount was significantly decreased as well in the SR membrane fraction. Thus, hypoxia results in the translocation of FKBP12.6 from the SR membrane to the cytosol (*i.e.*, dissociation of FKBP12.6 from RyRs) in PASMCs.

We next performed double immunofluorescence staining to further examine the effect of hypoxia on the association of FKBP12.6 with RyRs in intact PASMCs by analyzing their colocalization coefficient, an established means of quantifying the degree of colocalization between two molecules (11). The results indicate that the colocalization coefficient of FKBP12.6 with RyRs was largely decreased in hypoxic cells relative to normoxic cells (Fig. 1D), which validates the findings from the above-described *in vitro* experiments using isolated SR membrane and cytosolic factions.

FIG. 1. Hypoxia decreases the amount of FK506-binding protein 12.6 (FKBP12.6) on the sarcoplasmic reticulum (SR) membrane of pulmonary arteries (PAs), and increases the amount of FKBP12.6 in the cytosol. (**A**) Representative Western blots show FKBP12.6 and actin expression in isolated SR membrane and cytosol fractions from mouse PAs pretreated with normoxia or hypoxia for 5 min. (**B**) Bar graphs summarize the effect of hypoxia on the amount of FKBP12.6 in isolated SR membrane and cytosol fractions. FKBP12.6 levels are shown as the ratio to actin. Data presented were obtained from three independent experiments. $^*p < 0.05$ compared with normoxia. (**C**) Western blots exemplify expression of calnexin and actin in isolated SR membrane fraction. Bar graph illustrates the ratio of FKBP12.6 to calnexin amount in the SR membrane fraction. Data were collected from three separate experiments. $^*p < 0.05$ compared with normoxia. (**D**) Original images show double immunofluorescence staining of FKBP12.6 and ryanodine receptors (RyRs) in PA smooth muscle cells (PASMCs). RyRs and IP_3Rs were stained with a specific anti-FKBP12.6 and anti-RyR antibodies followed by Alex488- or Alex594-conjugated antibodies, respectively. Images were taken using an LSM510 confocal microscope. Bar graph quantifies the degree of colocalization of FKBP12.6 with RyRs by analyzing their colocalization coefficients. Data were obtained from nine cells $^*p < 0.05$ compared with normoxia. (For interpretation of the references to color in this figure legend, the reader is referred to the web version of this article at www.liebertonline.com/ars).

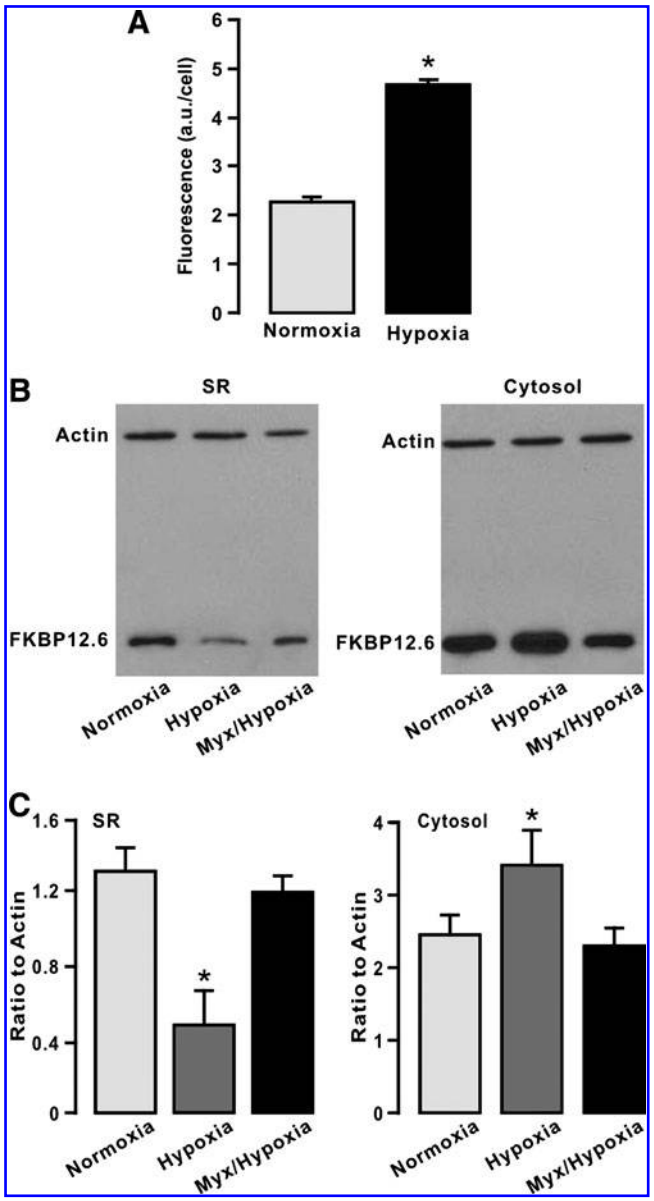

FIG. 2. Treatment with myxothiazol (Myx) to inhibit mitochondrial reactive oxygen species (ROS) generation prevents the hypoxic decrease in the amount of FKBP12.6 on the SR membrane of PAs and increase in the amount of FKBP12.6 in the cytosol. (**A**) Bar graph illustrates the effect of hypoxia on intracellular ROS generation, determined by 2,7-dichlorodihydrofluorescein fluorescence, in freshly isolated PASMCs. The 2,7-dichlorodihydrofluorescein fluorescence was expressed in arbitrary units (a.u.) per cell. $*p < 0.05$ compared with normoxia. (**B**) Representative Western blots of FKBP12.6 expression in isolated SR membrane and cytosol fractions from mouse PAs pretreated with normoxia for 5 min, hypoxia for 5 min, or Myx (10 μM) for 10 min followed by hypoxia for 5 min. (**C**) Summary of the effect of Myx on the hypoxic change in the amount of FKBP12.6 in isolated SR membrane and cytosol fractions from PAs. Data were taken from three separate experiments. $*p < 0.05$ compared with normoxia.

Inhibition of mitochondrial ROS generation blocks hypoxic translocation of FKBP12.6 from the SR membrane to the cytosol in PAs

Since mitochondrial ROS serve as important singling molecules in mediating hypoxic cellular responses in PASMCs (1, 24, 27), we presumed that inhibition of mitochondrial ROS generation could block the hypoxic responses. Consistent with our previous findings (17, 18, 23), here we further revealed that hypoxic exposure for 5 min resulted in a large increase in intracellular ROS generation, determined by the fluorescent ROS indicator DCF, in freshly isolated PASMCs (Fig. 2A). Application of myxothiazol (10 μM) for 10 min to inhibit mitochondrial ROS generation, as was previously reported (17, 18, 23), prevented hypoxia from decreasing the amount of FKBP12.6 in the SR membrane fraction of mouse PAs and increasing the amount of FKBP12.6 in the cytosol fraction (Fig. 2B and C).

It is known that Gpx1 is an important scavenger enzyme to metabolize mitochondrial and cytosolic H_2O_2 into water (24). To complement the above-described pharmacological study, thus, we employed Gpx1 gene overexpression and deletion mice to further assess the role of mitochondrial/cytosolic ROS in the hypoxic translocation of FKBP12.6. The results reveal that Gpx1 overexpression abolished the hypoxic reduction in the amount of FKBP12.6 in the SR membrane fraction of mouse PAs (Fig. 3). In contrast, Gpx1 gene deletion had an

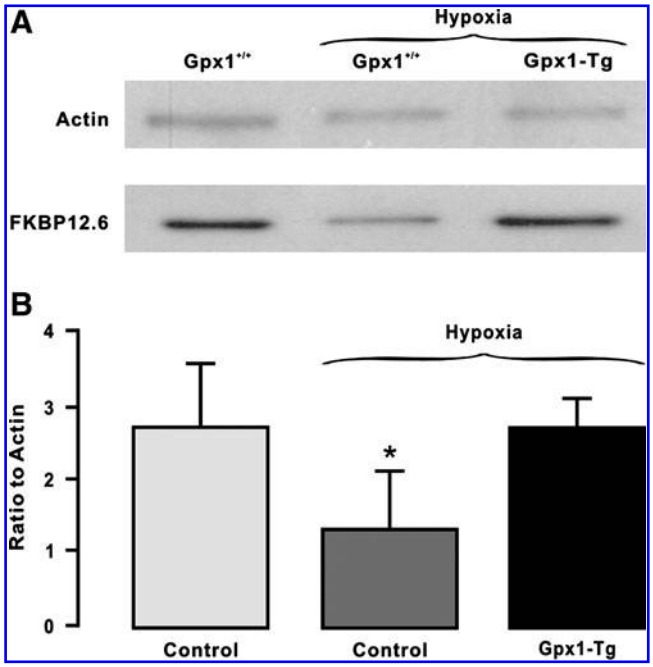

FIG. 3. Glutathione peroxidase-1 (Gpx1) gene overexpression to enhance mitochondrial/cytosolic H_2O_2 degradation blocks the hypoxic reduction in the amount of FKBP12.6 on the SR membrane of PAs. (**A**) Representative Western blots showing FKBP12.6 expression in isolated SR membrane fraction from control mouse PAs pretreated with normoxia or hypoxia for 5 min, or Gpx1 overexpressing mouse PAs pretreated with hypoxia for 5 min. (**B**) Summarized data of the effect of Gpx1 gene overexpression on the hypoxic reduction in the amount of FKBP12.6 in isolated SR membrane fraction from PAs. Data were obtained from three separate experiments. $*p < 0.05$ compared with normoxia.

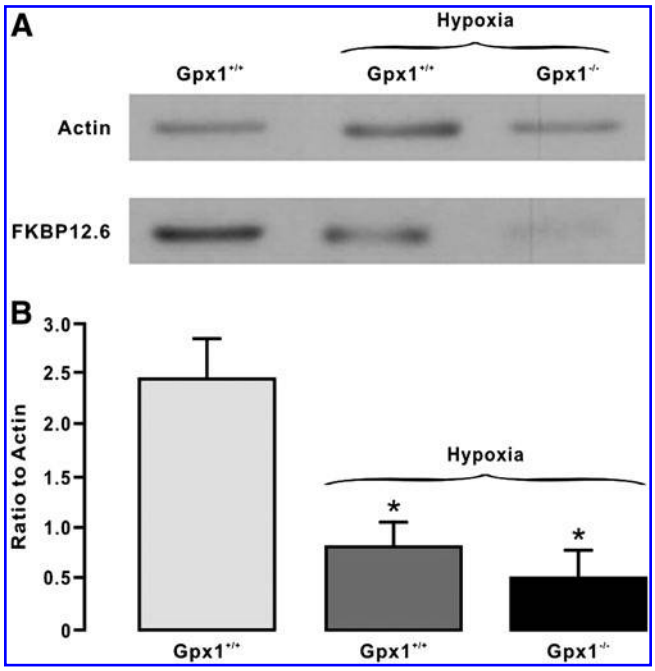

FIG. 4. Gpx1 gene deletion to inhibit mitochondrial/cytosolic H_2O_2 degradation mimics the hypoxic response, causing a decrease in the mount of FKBP12.6 on the SR membrane of PAs. (**A**) Representative Western blots of FKBP12.6 expression in isolated SR membrane fraction from control ($Gpx1^{+/+}$) and $Gpx1^{-/-}$ mouse PAs pretreated with normoxia or hypoxia for 5 min. (**B**) Summarized data illustrate the effect of Gpx1 gene overexpression on the hypoxic reduction in the amount of FKBP12.6 in isolated SR membrane fraction from PAs. Data were obtained from three separate experiments. $^*p < 0.05$ compared with normoxia.

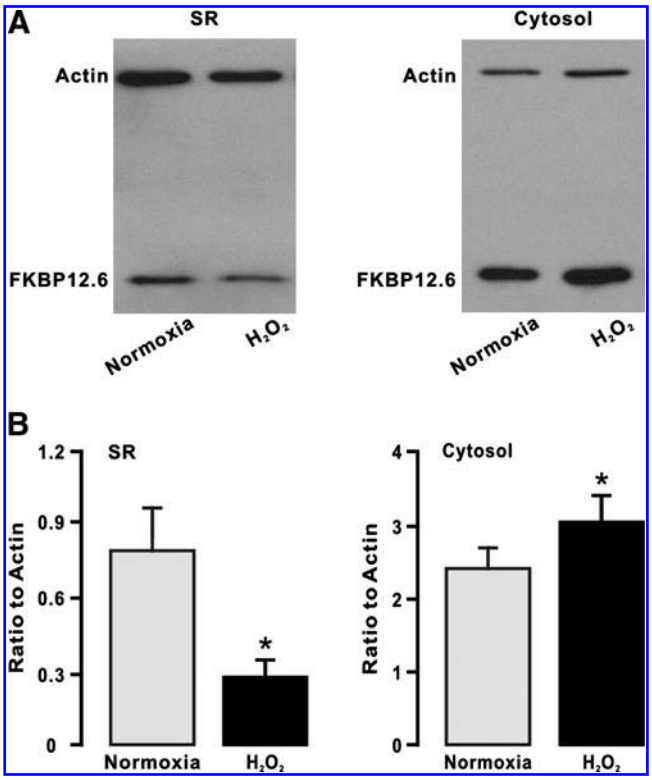

FIG. 5. H_2O_2 mimics the hypoxic response, reducing the amount of FKBP12.6 on the SR membrane of PAs. (**A**) Representative Western blots show FKBP12.6 expression in isolated SR membrane and cytosol fractions from mouse PAs pretreated with H_2O_2 (51 μM) for 5 min. (**B**) Summary of the effect of H_2O_2 on the amount of FKBP12.6 in isolated SR membrane and cytosol fractions from PAs. Data shown were obtained from three separate experiments. $^*p < 0.05$ compared with normoxia.

opposite effect (Fig. 4). Collectively, the increased generation of mitochondrial/cytosolic ROS may mediate the hypoxic translocation of FKBP12.6 from the SR membrane to the cytosol in PASMCs.

H_2O_2 mimics the hypoxic response, causing translocation of FKBP12.6 from the SR membrane to the cytosol in PAs

Since pharmacological and genetic inhibition of mitochondrial ROS generation can block the hypoxic translocation of FKBP12.6 from the SR membrane to the cytosol (Figs. 2 and 3), we proposed that exogenous ROS were able to mimic the hypoxic response. In support of this hypothesis, our data indicate that application of H_2O_2 (51 μM) for 5 min could decrease the amount of FKBP12.6 in the SR membrane fraction, whereas it could increase the amount of FKBP12.6 in the cytosol fraction (Fig. 5). These results provide further evidence that the hypoxic translocation of FKBP12.6 from the SR membrane to the cytosol is secondary to an increase in mitochondrial/cytosolic ROS generation in PASMCs.

Hypoxia results in FKBP12.6 oxidation leading to its dissociation from RyR2 on the SR membrane of PAs

Protein oxidation is one of the most important molecular mechanisms involved in ROS-mediated cellular responses. In view of this, we wondered whether hypoxia might cause FKBP12.6 oxidation leading to its translocation in PASMCs. As an example shown in Figure 6A, protein oxidation assay using an anti-DNP antibody against ROS-mediated, DNP-derivatized protein carbonyls did not detect oxidized FKBP12.6 in the SR membrane fraction of mouse PAs treated with either normoxia or hypoxia. However, re-blotting with an anti-FKBP antibody showed the presence of FKBP12.6. Similar results were obtained from three different experiments. In contrast, oxidized FKBP12.6 was found in the cytosol fraction of PAs treated with both normoxia and hypoxia. Moreover, remarkable oxidation of RyR2 protein was found in the SR membrane fraction of PAs treated with hypoxia but not with normoxia (Fig. 6B). These findings suggest that the hypoxic translocation of FKBP12.6 from the SR membrane to the cytosol may occur due to ROS-mediated oxidation of FKBP12.6, RyRs, or both in PASMCs.

We also conducted coimmunoprecipitation assay with a specific anti-RyR2 antibody to examine the hypoxic translocation of FKBP12.6. The results are shown in Figure 6C, in which the amount of FKBP12.6 immunoprecipitated by the anti-RyR2 antibody was significantly lower in the SR membrane fraction of mouse PAs treated with hypoxia than with normoxia. The mean amount of immunoprecipitated FKBP12.6 was decreased by 76% ($p < 0.05$, $n = 3$). Comparable

to hypoxia, application of exogenous H_2O_2 (51 μM) for 5 min could also largely reduce the amount of immunoprecipitated FKBP12.6 in the SR membrane fraction. Thus, hypoxia may dissociate FKBP12.6 from RyR2 in PASMCs by increasing intracellular ROS generation, leading to FKBP12.6 translocation from the SR membrane to cytosol.

FKBP12.6 removal enhances hypoxia- and H_2O_2-induced increase in $[Ca^{2+}]_i$ in PASMCs

Our previous study has shown that application of FK506 to chemically dissociate FKBP12.6 from RyRs and targeted gene deletion of FKBP12.6 both augment the hypoxic increase in $[Ca^{2+}]_i$ in PASMCs (30). Consonant with this previous report, here we found that application of FK506 (10 μM) largely enhanced the hypoxic Ca^{2+} response in freshly isolated PASMCs (Fig. 7A).

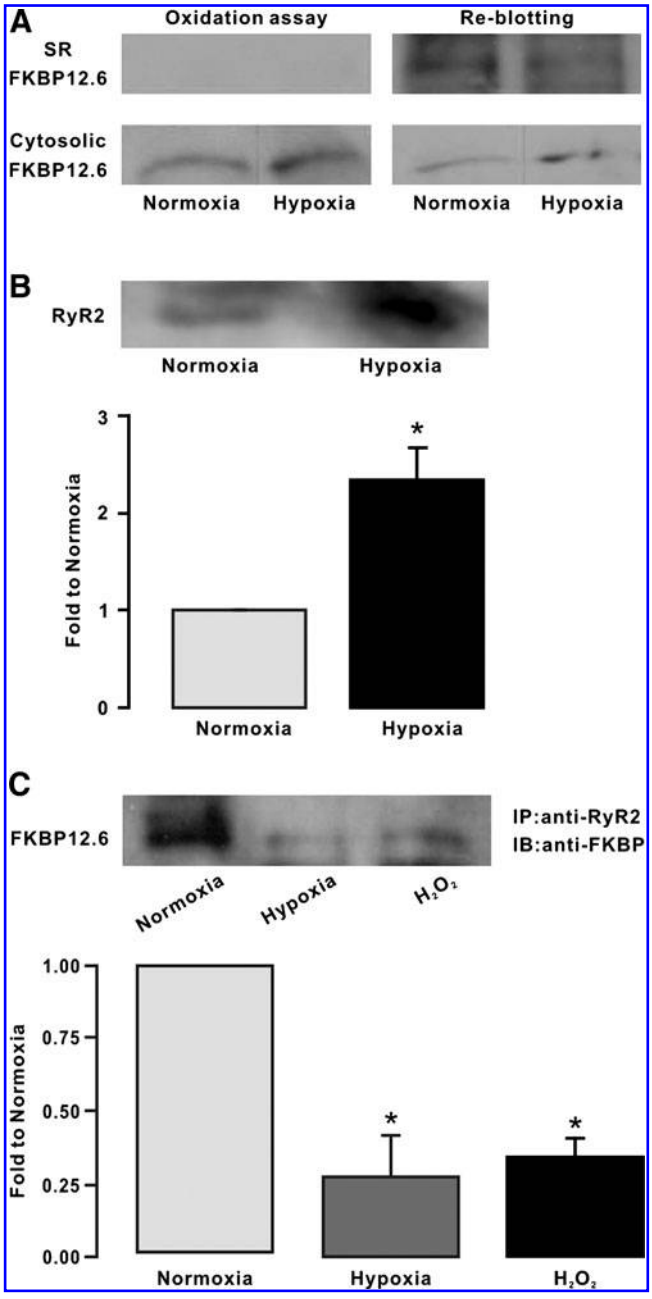

It is known that hypoxia causes an increase in background fluorescence (mainly from NADH) in rat PAs (6) and intact guinea pig hearts (2). Thus, we investigated whether hypoxia could alter background fluorescence to affect Ca^{2+} signals in isolated, single PASMCs. Similar to previous reports in vascular tissues and intact hearts (2, 6), we found that hypoxia induced a small increase in background fluorescence in isolated PAs (Fig. 7B). Similar results were observed in three different experiments. However, as an example shown in Figure 7C, hypoxia had no effect in isolated PASMCs ($n = 33$). As control, exogenous NADH (100 μM) resulted in a large increase in fluorescence. Thus, no significant background fluorescence was produced to affect the hypoxic Ca^{2+} signals in isolated PASMCs.

Since FKBP12.6 removal significantly enhances the hypoxic increase in $[Ca^{2+}]_i$ in isolated PASMCs (30) (Fig. 7A), we sought to examine the effect of FKBP12.6 removal on ROS-induced Ca^{2+} response. The results indicate that exogenous H_2O_2 induced a concentration-dependent increase in $[Ca^{2+}]_i$ in PASMCs (Fig. 7D). Importantly, FK506 exposure to dissociate FKBP12.6 from RyRs augmented H_2O_2-induced increase in $[Ca^{2+}]_i$.

Hypoxia increases the activity of RyR2 inducing Ca^{2+} release in PASMCs

The hypoxic dissociation of FKBP12.6 from RyR2 may perhaps augment the channel activity, leading to Ca^{2+} release from the SR in PASMCs. To provide the direct evidence for this perception, we scrutinized the effect of hypoxia on the activity of RyRs, determined using [^{3}H]-ryanodine binding assay (10). After hypoxic exposure, the maximal [^{3}H]-ryanodine binding to RyRs (B_{max}) was significantly increased in PAs relative to control (treated with normoxia) (Fig. 8A). Scatchard analysis of [^{3}H]-ryanodine binding indicate that the mean B_{max} in control and hypoxia-treated PAs was 0.09 ± 0.04 and 0.25 ± 0.04 pmol/mg protein, respectively ($p < 0.05, n = 5$)

FIG. 6. Hypoxia causes FKBP12.6 oxidation leading to its dissociation from type 2 ryanodine receptors (RyR2) on the SR membrane of PAs. (**A**) Representative Western blots of oxidized FKBP12.6 in isolated SR membrane and cytosol fractions from PAs pretreated with normoxia and hypoxia for 5 min. FKBP12.6 oxidation was assayed using an anti-2, 4-dinitrophenyl (DNP) antibody against ROS-mediated, DNP-derivatized protein carbonyls. Re-blotting of FKBP12.6 was performed using an anti-FKBP antibody. (**B**) Western blots show oxidation of immunoprecipitated RyR2, determined by examining ROS-mediated, DNP-derivatized protein carbonyls, in isolated SR membrane fraction from PAs pretreated with normoxia and hypoxia for 5 min. In the bar graph, the mean amount of immunoprecipitated oxidized RyR2 proteins in isolated SR membrane fraction from normoxic and hypoxic PAs were obtained from six different experiments. *$p < 0.05$ compared with normoxia. (**C**) Immunoprecipitation and Western blotting of FKBP12.6 in isolated SR membrane fraction from PAs pretreated with normoxia, hypoxia, and H_2O_2 (51 μM) for 5 min. FKBP12.6 was immunoprecipitated with an anti-RyR2 antibody and then immunoblotted with an anti-FKBP antibody. Bar graph summarizes the effect of hypoxia and H_2O_2 on the amount of FKBP12.6 in isolated SR membrane fraction of PAs. FKBP12.6 levels are shown as the ratio to normoxia. Data were taken from three separate experiments. *$p < 0.05$ compared with normoxia.

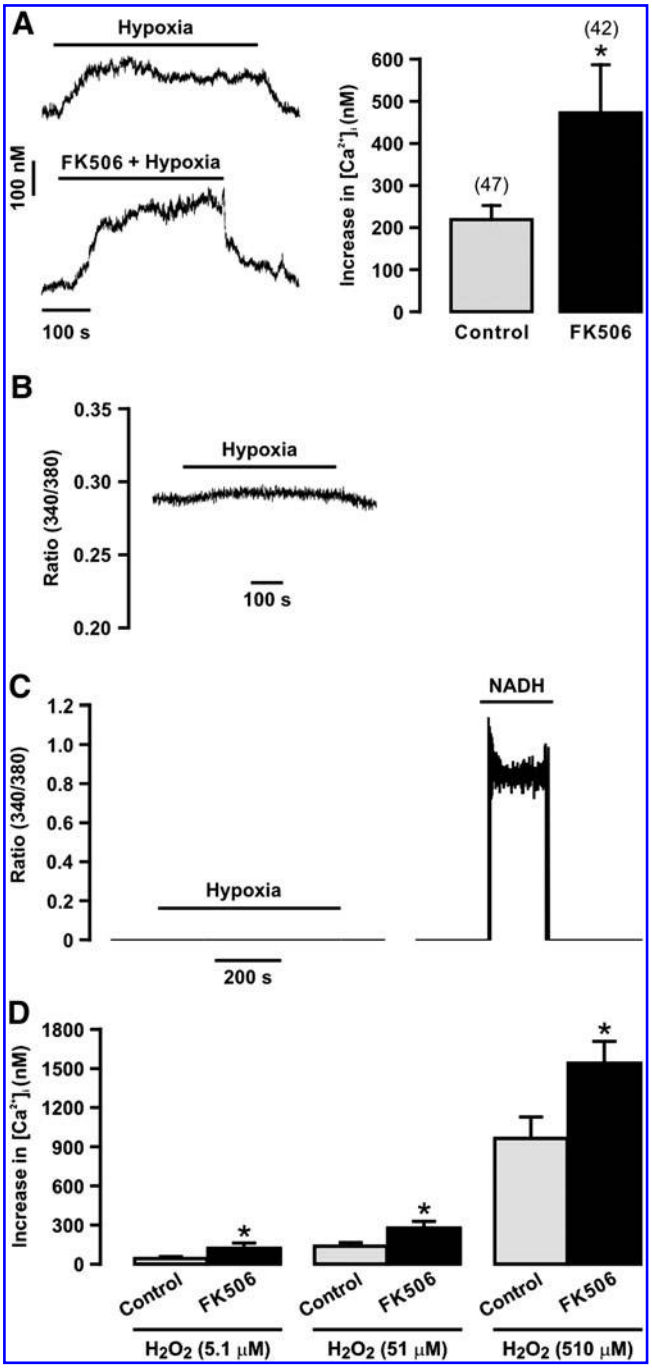

FIG. 7. Removal of FKBP12.6 with FK506 exposure enhances hypoxia- and H_2O_2-induced increase $[Ca^{2+}]_i$ in PASMCs. Original recordings show a hypoxic increase in $[Ca^{2+}]_i$ in a PASMC in the absence and presence of FK506 (10 μM). Bar graph summarizes the effect of FK506 on the hypoxic increase in $[Ca^{2+}]_i$. Numbers in parentheses indicate the number of tested cells from three different mice. $^*p < 0.05$ compared with control (in the absence of FK506). (**B**) An original recording of the effect of hypoxia on background fluorescence (ratio of 340/380) in a mouse PA. (**C**) Original recordings show the effect of hypoxia (*left*) and NADH (100 μM, *right*) on background fluorescence in a mouse PASMCs. (**D**) Graph shows H_2O_2-induced increase in $[Ca^{2+}]_i$ in mouse PASMCs in the absence (control) and presence of FK506 (10 μM). Data were obtained from 42 cells in the absence FK506 and 38 cells in the presence of FK506. $^*p < 0.05$ compared with control.

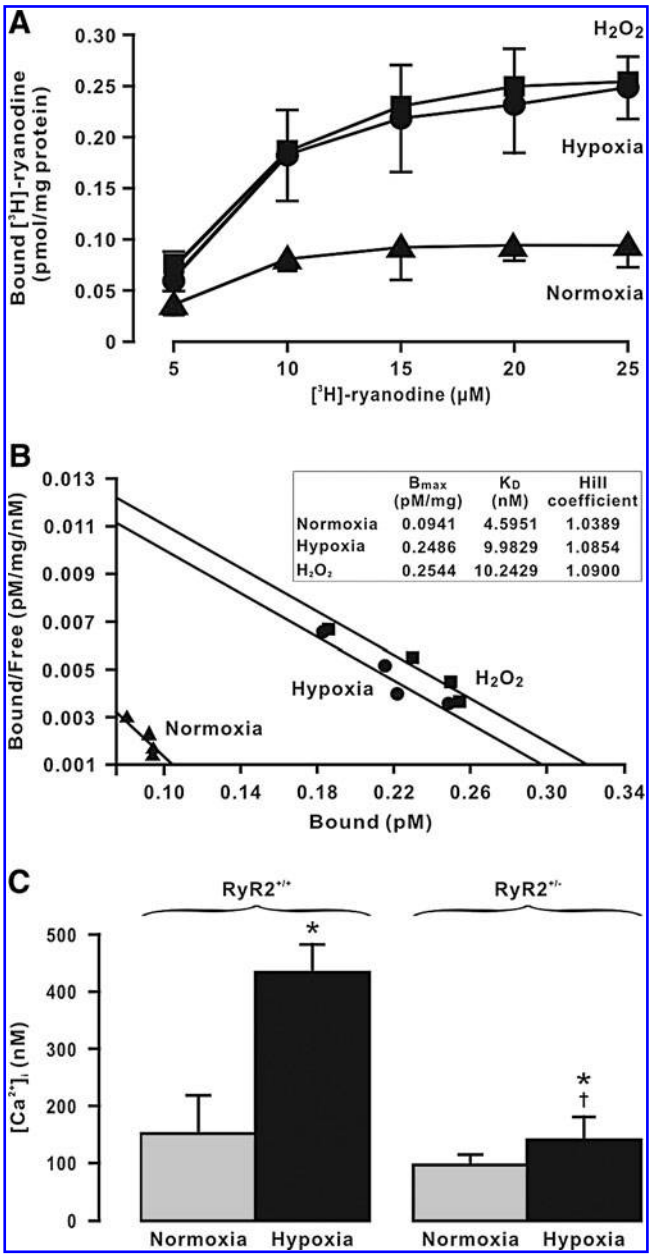

FIG. 8. Hypoxia increases the activity of RyR2 inducing intracellular Ca^{2+} release in PASMCs. (**A**) [^{3}H]-ryanodine binding assays were conducted in cell lysates from mouse PAs pretreated with normoxia, hypoxia, and H_2O_2 (51 μM) for 5 min. Data were obtained from three different experiments. (**B**) Scatchard analysis of [^{3}H]-ryanodine binding in cell lysates from mouse PAs pretreated with normoxia, hypoxia, and H_2O_2 were performed to determine B_{max}, K_D, and Hill coefficient. (**C**) Graph shows the hypoxia-induced increase in $[Ca^{2+}]_i$ in $RyR2^{+/+}$, and $RyR2^{-/+}$ mouse PASMCs. Data were obtained from five independent experiments. $^*p < 0.05$ compared with normoxia (before hypoxia); $^\dagger p < 0.05$ compared with $RyR2^{+/+}$/hypoxia.

(Fig. 8B). Hypoxic exposure also increased the apparent affinity of [^{3}H]-ryanodine binding to RyRs (K_D), but it did not alter the Hill coefficient. Analogous to hypoxia, pretreatment with H_2O_2 (51 μM) for 5 min also augmented both B_{max} and K_D without affecting the Hill coefficient.

Next, we further determined whether hypoxia could augment the activity of RyR2 by specifically assessing the effect of RyR2 gene deletion on the hypoxia-induced increase in $[Ca^{2+}]_i$ in PASMCs. Hypoxic exposure for 5 min caused a large increase in $[Ca^{2+}]_i$ in freshly isolated PASMCs from control ($RyR2^{+/+}$) mice. As summarized in Figure 8C, the mean $[Ca^{2+}]_i$ before (normoxia) and after hypoxic exposure was 146.9 ± 31.1 and 425.6 ± 81.7 *nM*, respectively ($n = 6$, $p < 0.05$). Importantly, the hypoxic increase in $[Ca^{2+}]_i$ was blocked in cells from $RyR2^{-/+}$ mice. These observations further indicate that hypoxia results in the increased activity of RyR2 leading to intracellular Ca^{2+} release in PASMCs.

Discussion

The functional importance of FKBP12.6 in the regulation of RyRs activity and associated intracellular Ca^{2+} homeostasis has been well recognized in cardiac myocytes (28). We and other investigators have recently shown that FKBP12.6 is associated with RyR2 and inhibits the activity of these Ca^{2+} release channels in vascular SMCs (20, 30). Moreover, chemical and genetic removal of this RyR2-associated protein significantly enhances the hypoxia-induced increase in $[Ca^{2+}]_i$ in PASMCs and HPV (30). These previous findings suggest that hypoxia may possibly cause dissociation of FKBP12.6 from RyR2 followed by the increased channel activity, contributing to hypoxic cellular responses in PASMCs. For the first time, here we have provided biochemical evidence demonstrating that after hypoxic exposure for 5 min, the amount of FKBP12.6 is significantly decreased on the SR membrane of PAs and correspondingly increased in the cytosol (Fig. 1). In addition, hypoxia has no effect on FKBP12.6 expression level. These data support our hypothesis that FKBP12.6 is dissociated with RyR2 in PASMCs during hypoxic stimulation. Our double immunofluorescence staining experiments reveal that the association of FKBP12.6 with RyRs in intact PASMCs is significantly reduced as well after hypoxic stimulation, as determined by a decrease in their colocalization coefficient. These results further validate the findings from *in vitro* experiments using isolated SR membrane and cytosolic fractions.

Previous studies from our and other laboratories have shown that mitochondrial ROS serve as initial molecules in the mediation of the hypoxic increase in $[Ca^{2+}]_i$ in PASMCs (1, 24, 27). As such, we wondered whether the hypoxic dissociation of FKBP12.6 from RyRs was likely to be secondary to the increased mitochondrial ROS generation. In agreement with our previous findings (17, 18, 23), in this study we have further found that hypoxia results in a large increase in intracellular ROS generation in PASMCs (Fig. 2). Treatment with myxothiazol, an archetypical inhibitor of mitochondrial ROS generation, prevents hypoxia from causing a decrease in the amount of FKBP12.6 on the SR membrane of PAs and an increase in FKBP12.6 in the cytosol. Complementing the pharmacological data, genetic inhibition of mitochondrial/cytosolic ROS generation by overexpression of the Gpx1 gene blocks the hypoxic decrease of FKBP12.6 on the SR membrane (Fig. 3). Gpx1 gene deletion to augment mitochondrial/cytosolic ROS generation, similar to hypoxia, results in a decrease in the amount of FKBP12.6 on the SR membrane (Fig. 4). We have also found that the hypoxic response is abolished in $Gpx1^{-/-}$ PAs. Consistent with these pharmacological and genetic effects, exogenous H_2O_2, mimicking the hypoxic response, leads to a decrease in the amount of FKBP12.6 on the SR membrane and an increase in the amount of FKBP12.6 in the cytosol (Fig. 5). All these observations, together with well-documented findings that hypoxia increases mitochondrial ROS generation mediating Ca^{2+} and contractile responses (1, 24, 27), insinuate that the hypoxic removal of FKBP12.6 from RyRs on the SR membrane is due to the increased generation of mitochondrial ROS in PASMCs.

We have shown that oxidized FKBP12.6 is detected in the cytosol but not on the SR membrane under both normoxic and hypoxic conditions, although re-blotting assessments show that FKBP12.6 is present on the SR membrane and in the cytosol (Fig. 6). The significant oxidation of RyR2 is observed on the SR membrane after hypoxic but not normoxic exposure. Hypoxia may increase mitochondrial/cytosolic ROS generation to oxidize FKBP12.6 on the SR membrane. The oxidized protein would then dissociate with RyRs on the SR membrane. On the other hand, ROS may possibly oxidize unbound FKBP12.6 in the cytosol; as such, the oxidized FKBP12.6 cannot bind to RyR2 on the SR membrane. Zissimopoulos *et al.* have reported that H_2O_2 results in the diminished FKBP12.6-RyR2 binding in cardiac myocytes (33). Moreover, these authors have also found that cysteine-null mutant FKBP12.6 retains H_2O_2-sensitive interaction with RyR2, whereas FKBP12.6 binding is decreased by $\sim 25\%$ when RyR2 has been pretreated with H_2O_2. Thus, it would be interesting to determine the potential role of these and other redox-sensitive residues in FKBP12.6 in the hypoxic dissociation of FKBP12.6 from RyR2 in PASMCs. Consistent with the ROS-dependent, hypoxic translocation of FKBP12.6, our FKBP12.6 immunoprecipitation assays with a specific anti-RyR2 antibody further reveal that the amount of FKBP12.6 on the SR membrane is significantly reduced after hypoxic exposure. Similarly, application of H_2O_2 decreases the amount of immunoprecipitated FKBP12.6 as well.

Since FKBP12.6 functions as an endogenous inhibitor of RyR2 in vascular SMCs (20, 30), hypoxic removal of this protein may increase the activity of RyR2. Supportively, our previous study has found that chemical and genetic removal of this protein enhance both the hypoxic increase in $[Ca^{2+}]_i$ and contraction in PASMCs (30). In agreement with these previous findings, here we have further shown that application of FK506 to chemically remove FKBP12.6 leads to a larger increase in $[Ca^{2+}]_i$ in PASMCs (Fig. 7). It has been reported that hypoxia can produce an increase in background fluorescence (mainly from NADH) to affect the hypoxic Ca^{2+} signal in vascular tissues and intact hearts (2, 6). Similar to these previous reports, we have also found the hypoxic increase in background fluorescence in PAs. In contrast, hypoxia has no effect in PASMCs. Thus, the hypoxic Ca^{2+} signal observed in PASMCs is not affected by background fluorescence. The reason for the different effect of hypoxia on background fluorescence in multicellular PAs and single PASMCs is unclear. However, we speculate that hypoxia may perhaps cause a small amount of NADH accumulated in the cytosol and extracellular space in PAs to produce detectable fluorescence, whereas NADH cannot be built up to generate detectable fluorescence in single PASMCs, because it consistently leaks out of the cells. Since the ROS-dependent dissociation of FKBP12.6 from RyR2 mediates the hypoxic increase in $[Ca^{2+}]_i$ in PASMCs, we wondered whether FKBP12.6

removal could, in parallel, enhance ROS-induced Ca^{2+} response. Our data reveal that chemical removal of FKBP12.6 with FK506 exposure significantly augments H_2O_2-evoked concentration-dependent increase in $[Ca^{2+}]_i$ as well in PASMCs. Further, our previous study has shown that FKBP12.6 removal directly induces Ca^{2+} release in PASMCs (30). Taken together, hypoxia removes FKBP12.6 from RyR2 *via* ROS signaling to open the RyR2 channels, contributing to the hypoxic increase in $[Ca^{2+}]_i$ in PASMCs.

In reinforcement of the concept that hypoxia causes ROS-dependent dissociation of FKBP12.6 from RyR2 to cause the channel opening in PASMCs, we have further shown that hypoxia can significantly augment both the maximal and apparent affinity of [^{3}H]-ryanodine binding to RyRs (Fig. 8). Application of exogenous H_2O_2 produces similar effects. The hypoxic increase in $[Ca^{2+}]_i$ is almost completely abolished in $RyR2^{-/+}$ PASMCs. One may perhaps wonder why heterogeneous (partial) RyR2 gene deletion fully, rather partially blocks the hypoxic response. We do not have a specific answer for this question yet, but we can speculate that the decreased expression levels of RyR2 by heterogeneous gene deletion may cause the inability of the remaining channel molecules to form the functional Ca^{2+} release units; as such, hypoxia is no longer able to induce a typical cellular response in $RyR2^{-/+}$ PASMCs. Interestingly, membrane depolarization does not trigger normal Ca^{2+} release from the SR in $RyR2^{-/+}$ airway SMCs (9). We have previously reported that both RyR1 and RyR3 gene deletion greatly inhibit the hypoxic increase in $[Ca^{2+}]_i$ in PASMCs (7, 32). These results, together with the finding that hypoxia is all but incapable of inducing an increase in $[Ca^{2+}]_i$ in $RyR2^{-/+}$ cells (in this study), suggest that RyR2 may form structural and/or functional Ca^{2+} release units with RyR1 and RyR3. In support of this view, heterologously expressed RyR2 has been found to be able to interact physically and biologically with RyR1 and RyR3 in HEK293 cells (29). Due to the formation of these mixed Ca^{2+} release units, RyR1, RyR2, and RyR3 are all involved in hypoxic Ca^{2+} responses in PASMCs. Thus, it is not surprising that targeted gene deletion of each of individual RyR subtypes can block the hypoxic increase in $[Ca^{2+}]_i$ in PASMCs.

A recent, elegant study has disclosed that oxidative modifications of RyR2 enhance the channel activity, leading to Ca^{2+} release in cardiac cells (21). Here, we have provided experimental evidence to show that hypoxia causes oxidation of RyR2 in PASMCs (Fig. 6). Thus, it is likely that in addition to ROS-dependent dissociation of FKBP12.6 from RyR2, oxidation of RyR2 may also play an important role in the hypoxic increase in $[Ca^{2+}]_i$ in PASMCs. In support of this likelihood, both hypoxia- and H_2O_2-induced Ca^{2+} responses are augmented in PASMCs after chemical and genetic removal FKBP12.6 (Fig. 7) (30). Moreover, neurotransmitter-evoked Ca^{2+} release is enhanced as well in PASMCs deficient of FKBP12.6 (30). Accordingly, hypoxia can not only cause ROS-mediated dissociation of FKBP12.6 to eliminate its inhibitory effect on the RyR2 channels, but it may also lead to ROS-dependent oxidation of RyR2 to enhance the channel activity, mediating the hypoxic increase in $[Ca^{2+}]_i$ in PASMCs.

In conclusion, the present study, for the first time, provides biochemical and genetic evidence that acute hypoxia leads to the dissociation of FKBP12.6 from RyR2 in PASMCs. The hypoxic dissociation of FKBP12.6, which is secondary to an increase in mitochondrial/cytosolic ROS generation, can significantly augment the activity of RyR2, contributing to the hypoxic increase in $[Ca^{2+}]_i$ in PASMCs. Hypoxia causes large vasoconstriction in pulmonary but not in systemic (*e.g.*, mesenteric and cerebral) arteries (24); thus, further studies are necessary to determine the ROS-mediated dissociation of FKBP12.6 from RyRs in the heterogeneity of hypoxic cellular responses in PA and systemic artery.

Acknowledgments

This work was supported by the NIH R01HL64043, R01HL064043-S1, and R01HL075190 (Y.-X.W.), as well as AHA EIA0340160N (Y.-X.W.) and SDG0630236N (Y.-M.Z.). The authors thank Ms. Amanda Belawski and Rachel Würster for their excellent technical assistance.

Author Disclosure Statement

None of the authors has a financial interest in the subject of this article.

References

1. Archer SL, Gomberg-Maitland M, Maitland ML, Rich S, Garcia JG, and Weir EK. Mitochondrial metabolism, redox signaling, and fusion: a mitochondria-ROS-HIF-1α-Kv1.5 O_2-sensing pathway at the intersection of pulmonary hypertension and cancer. *Am J Physiol Heart Circ Physiol* 294: H570–H578, 2008.
2. Brachmanski M, Gebhard MM, and Nobiling R. Separation of fluorescence signals from Ca^{2+} and NADH during cardioplegic arrest and cardiac ischemia. *Cell Calcium* 35: 381–391, 2004.
3. Dipp M, Nye PC, and Evans AM. Hypoxic release of calcium from the sarcoplasmic reticulum of pulmonary artery smooth muscle. *Am J Physiol Lung Cell Mol Physiol* 281: L318–L325, 2001.
4. Jabr RI, Toland H, Gelband CH, Wang XX, and Hume JR. Prominent role of intracellular Ca^{2+} release in hypoxic vasoconstriction of canine pulmonary artery. *Br J Pharmacol* 122: 21–30, 1997.
5. Lauderback CM, Hackett JM, Keller JN, Varadarajan S, Szweda L, Kindy M, Markesbery WR, and Butterfield DA. Vulnerability of synaptosomes from apoE knock-out mice to structural and oxidative modifications induced by A β(1–40): implications for Alzheimer's disease. *Biochemistry* 40: 2548–2554, 2001.
6. Leach RM, Hill HM, Snetkov VA, Robertson TP, and Ward JP. Divergent roles of glycolysis and the mitochondrial electron transport chain in hypoxic pulmonary vasoconstriction of the rat: identity of the hypoxic sensor. *J Physiol* 536: 211–224, 2001.
7. Li XQ, Zheng YM, Rathore R, Ma J, Takeshima H, and Wang YX. Genetic evidence for functional role of ryanodine receptor 1 in pulmonary artery smooth muscle cells. *Pflugers Arch* 457: 771–783, 2009.
8. Lin MJ, Yang XR, Cao YN, and Sham JS. Hydrogen peroxide-induced Ca^{2+} mobilization in pulmonary arterial smooth muscle cells. *Am J Physiol Lung Cell Mol Physiol* 292: L1598–L1608, 2007.
9. Liu QH, Zheng YM, Korde AS, Yadav VR, Rathore R, Wess J, and Wang YX. Membrane depolarization causes a direct activation of G protein-coupled receptors leading to local Ca^{2+} release in smooth muscle. *Proc Natl Acad Sci U S A* 106: 11418–11423, 2009.
10. Liu Z, Zhang J, Li P, Chen SR, and Wagenknecht T. Three-dimensional reconstruction of the recombinant type 2

ryanodine receptor and localization of its divergent region 1. *J Biol Chem* 277: 46712–46719, 2002.
11. Manders EM, Verbeek FJ, and Aten JA. Measurement of colocalization of objects in dual-color confocal images. *J Microsc* 169: 375–382, 1993.
12. Morio Y and McMurtry IF. Ca^{2+} release from ryanodine-sensitive store contributes to mechanism of hypoxic vasoconstriction in rat lungs. *J Appl Physiol* 92: 527–534, 2002.
13. Ng LC, Wilson SM, and Hume JR. Mobilization of sarcoplasmic reticulum stores by hypoxia leads to consequent activation of capacitative Ca^{2+} entry in isolated canine pulmonary arterial smooth muscle cells. *J Physiol* 563: 409–419, 2005.
14. Ng LC, Wilson SM, McAllister CE, and Hume JR. Role of InsP3 and ryanodine receptors in the activation of capacitative Ca^{2+} entry by store depletion or hypoxia in canine pulmonary arterial smooth muscle cells. *Br J Pharmacol* 152: 101–111, 2007.
15. Post JM, Gelband CH, and Hume JR. $[Ca^{2+}]_i$ inhibition of K^+ channels in canine pulmonary artery. Novel mechanism for hypoxia-induced membrane depolarization. *Circ Res* 77: 131–139, 1995.
16. Pourmahram GE, Snetkov VA, Shaifta Y, Drndarski S, Knock GA, Aaronson PI, and Ward JP. Constriction of pulmonary artery by peroxide: role of Ca^{2+} release and PKC. *Free Radic Biol Med* 45: 1468–1476, 2008.
17. Rathore R, Zheng YM, Li XQ, Wang QS, Liu QH, Ginnan R, Singer HA, Ho YS, and Wang YX. Mitochondrial ROS-PKCε signaling axis is uniquely involved in hypoxic increase in $[Ca^{2+}]_i$ in pulmonary artery smooth muscle cells. *Biochem Biophys Res Commun* 351: 784–790, 2006.
18. Rathore R, Zheng YM, Niu CF, Liu QH, Korde A, Ho YS, and Wang YX. Hypoxia activates NADPH oxidase to increase [ROS](i) and $[Ca^{2+}]_i$ through the mitochondrial ROS-PKCε signaling axis in pulmonary artery smooth muscle cells. *Free Radic Biol Med* 45: 1223–1231, 2008.
19. Salvaterra CG and Goldman WF. Acute hypoxia increases cytosolic calcium in cultured pulmonary arterial myocytes. *Am J Physiol* 264: L323–L328, 1993.
20. Tang WX, Chen YF, Zou AP, Campbell WB, and Li PL. Role of FKBP12.6 in cADPR-induced activation of reconstituted ryanodine receptors from arterial smooth muscle. *Am J Physiol Heart Circ Physiol* 282: H1304–H1310, 2002.
21. Terentyev D, Gyorke I, Belevych AE, Terentyeva R, Sridhar A, Nishijima Y, de Blanco EC, Khanna S, Sen CK, Cardounel AJ, Carnes CA, and Gyorke S. Redox modification of ryanodine receptors contributes to sarcoplasmic reticulum Ca^{2+} leak in chronic heart failure. *Circ Res* 103: 1466–1472, 2008.
22. Vandier C, Delpech M, and Bonnet P. Spontaneous transient outward currents and delayed rectifier K^+ current: effects of hypoxia. *Am J Physiol* 275: L145–L154, 1998.
23. Wang QS, Zheng YM, Dong L, Ho YS, Guo Z, and Wang YX. Role of mitochondrial reactive oxygen species in hypoxia-dependent increase in intracellular calcium in pulmonary artery myocytes. *Free Radic Biol Med* 42: 642–653, 2007.
24. Wang YX and Zheng YM. ROS-dependent signaling mechanisms for hypoxic Ca^{2+} responses in pulmonary artery myocytes. *Antioxid Redox Signal* 12: 611–623, 2010.
25. Wang YX, Zheng YM, Abdullaev II, and Kotlikoff MI. Metabolic inhibition with cyanide induces intracellular calcium release in pulmonary artery myocytes and *Xenopus* oocytes. *Am J Physiol Cell Physiol* 284: C378–C388, 2003.
26. Waypa GB, Marks JD, Mack MM, Boriboun C, Mungai PT, and Schumacker PT. Mitochondrial reactive oxygen species trigger calcium increases during hypoxia in pulmonary arterial myocytes. *Circ Res* 91: 719–726, 2002.
27. Waypa GB and Schumacker PT. Oxygen sensing in hypoxic pulmonary vasoconstriction: using new tools to answer an age-old question. *Exp Physiol* 93: 133–138, 2008.
28. Wehrens XH, Lehnart SE, and Marks AR. Intracellular calcium release and cardiac disease. *Annu Rev Physiol* 67: 69–98, 2005.
29. Xiao B, Masumiya H, Jiang D, Wang R, Sei Y, Zhang L, Murayama T, Ogawa Y, Lai FA, Wagenknecht T, and Chen SR. Isoform-dependent formation of heteromeric Ca^{2+} release channels (ryanodine receptors). *J Biol Chem* 277: 41778–41785, 2002.
30. Zheng YM, Mei QB, Wang QS, Abdullaev I, Lai FA, Xin HB, Kotlikoff MI, and Wang YX. Role of FKBP12.6 in hypoxia- and norepinephrine-induced Ca^{2+} release and contraction in pulmonary artery myocytes. *Cell Calcium* 35: 345–355, 2004.
31. Zheng YM, Wang QS, Liu QH, Rathore R, Yadav V, and Wang YX. Heterogeneous gene expression and functional activity of ryanodine receptors in resistance and conduit pulmonary as well as mesenteric artery smooth muscle cells. *J Vasc Res* 45: 469–479, 2008.
32. Zheng YM, Wang QS, Rathore R, Zhang WH, Mazurkiewicz JE, Sorrentino V, Singer HA, Kotlikoff MI, and Wang YX. Type-3 ryanodine receptors mediate hypoxia-, but not neurotransmitter-induced calcium release and contraction in pulmonary artery smooth muscle cells. *J Gen Physiol* 125: 427–440, 2005.
33. Zissimopoulos S, Docrat N, and Lai FA. Redox sensitivity of the ryanodine receptor interaction with FK506-binding protein. *J Biol Chem* 282: 6976–6983, 2007.

Address correspondence to:
Dr. Yong-Xiao Wang
Center for Cardiovascular Sciences (MC-8)
Albany Medical College
47 New Scotland Ave.
Albany, NY 12208

E-mail: WangY@mail.amc.edu

Date of first submission to ARS Central, December 9, 2009; date of final revised submission, May 8, 2010; date of acceptance, June 2, 2010.

Abbreviations Used

BSA = bovine serum albumin
DCF = 2,7-dichlorodihydrofluorescein
DNPH = 2, 4-dinitrophenyl hydrazine
FKBP = FK506-binding protein
Gpx1 = glutathione peroxidase 1
HPV = hypoxic pulmonary vasoconstriction
PA = pulmonary artery
PASMCs = pulmonary artery smooth muscle cells
PBS = phosphate-buffered saline
PSS = physiological saline solution
PVDF = polyvinylidene fluoride
ROS = reactive oxygen species
RyR = ryanodine receptor
RyR2 = type 2 ryanodine receptors
SDS-PAGE = sodium dodecyl sulfate–polyacrylamide gel electrophoresis
SMCs = smooth muscle cells
SR = sarcoplasmic reticulum
TBST = Tris-buffered saline with Tween-20

This article has been cited by:

1. Eberhard Schulz , Philip Wenzel , Thomas Münzel , Andreas Daiber . Mitochondrial Redox Signaling: Interaction of Mitochondrial Reactive Oxygen Species with Other Sources of Oxidative Stress. *Antioxidants & Redox Signaling*, ahead of print. [Abstract] [Full Text HTML] [Full Text PDF] [Full Text PDF with Links]
2. Amit S. Korde, Vishal R. Yadav, Yun-Min Zheng, Yong-Xiao Wang. 2011. Primary role of mitochondrial Rieske iron–sulfur protein in hypoxic ROS production in pulmonary artery myocytes. *Free Radical Biology and Medicine* **50**:8, 945-952. [CrossRef]